Published in final edited form as:

Dev Biol. 2016 July 1; 415(1): 87–97. doi:10.1016/j.ydbio.2016.04.018.

Cell death regulates muscle fiber number

Tatevik Sarkissian[1], **Richa Arya**[1], **Seda Gyonjyan**[1], **Barbara Taylor**[2], and **Kristin White**[1,*]

[1]CBRC, Massachusetts General Hospital Research Institute/Harvard Medical School, Boston, MA 02129, USA

[2]Department of Integrative Biology, Oregon State University, Corvallis, OR 97331, USA

Abstract

Cell death can have both cell autonomous and non-autonomous roles in normal development. Previous studies have shown that the central cell death regulators *grim* and *reaper* are required for the developmentally important elimination of stem cells and neurons in the developing central nervous system (CNS). Here we show that cell death in the nervous system is also required for normal muscle development. In the absence of *grim* and *reaper*, there is an increase in the number of fibers in the ventral abdominal muscles in the Drosophila adult. This phenotype can be partially recapitulated by inhibition of cell death specifically in the CNS, indicating a non-autonomous role for neuronal death in limiting muscle fiber number. We also show that FGFs produced in the cell death defective nervous system are required for the increase in muscle fiber number. Cell death in the muscle lineage during pupal stages also plays a role in specifying fiber number. Our work suggests that FGFs from the CNS act as a survival signal for muscle FCs. Thus, proper muscle fiber specification requires cell death in both the nervous system and in the developing muscle itself.

Keywords

Drosophila; muscle; apoptosis; FGF

Introduction

Programmed cell death is a prevalent and important cell fate in the development of multicellular organisms (Arya and White, 2015). Accurate regulation of both proliferation and cell death is essential to control cell number in developing tissues. The selective death of cells is also necessary for the precise organization of tissues, such as matching neuronal inputs to their targets, or to pattern sensory organs such as the eye. Although the presence of apoptotic cells is detected in many developing tissues, the importance of cell death in the normal development of most tissues has not been extensively studied.

*Corresponding author: K White, CBRC, Massachusetts General Hospital Research Institute, Bldg. 149, 13th St, Charlestown, MA 02129, USA. Tel: +1 617 726 4440; Fax +1 617 726 4453; kristin.white@mgh.harvard.edu.

Drosophila provides a particularly strong model system to examine the role of apoptosis in development, as the central regulators of cell death in development are known, and their activity can be manipulated genetically (Arya and White, 2015). Here we focus on the role of cell death in Drosophila adult muscle development. Loss of muscle tissue is an important pathology in human disease, and studies in Drosophila have the potential to provide mechanistic insights into how muscle death is regulated (Piccirillo et al., 2014).

Muscle development in Drosophila occurs in two stages (Schejter and Baylies, 2010). In the embryo, muscles consist of single multinucleated fibers that form in a stereotyped pattern. Each muscle originates with a founder cell, which determines muscle identity. Fusion-competent myoblasts fuse with the founder cell, resulting in elongation and formation of the mature larval muscles. Adult muscle development occurs in the pupae. In contrast to larval muscles, adult muscles consist of multiple fibers. Adult muscle precursors, set aside during embryonic life, proliferate to become the myoblasts of the adult musculature (Broadie and Bate, 1991). Adult muscles are specified in two ways (Atreya and Fernandes, 2008). Some adult muscles are templated by pre-existing larval muscles. These muscles grow through the fusion of additional myoblasts during pupal life. Other muscles, such as the body wall muscles, are formed *de novo* from adult specific FCs. In these muscles, the formation of each fiber is initiated by a single founder cell, which then fuses with additional myoblasts to form a mature fiber (Dutta et al., 2004).

Innervation plays a differing role in embryonic and adult muscle development. In the embryo, muscle formation precedes and occurs independently of innervation (Bate, 1990). In contrast, formation of adult body wall muscles occurs simultaneously with innervation, and myoblasts migrate to their final destination along nerve pathways (Bate et al., 1991). In the absence of innervation, patterning of most adult muscles is normal. However, the number and size of fibers is reduced (Currie and Bate, 1995).

Major muscle groups in the adult include appendage muscles, thoracic flight muscles, and abdominal body wall muscles. The repetitive and simple organization of the abdominal muscles provides a particularly tractable model for examining alterations in adult myogenesis (Hebbar et al., 2006). The tissue is accessible in both pupae and adults, and extensive studies have described the normal development of these muscles (Bate et al., 1991; Currie and Bate, 1995; Dutta et al., 2004). Adult abdominal body wall muscles consist of dorsal muscles, ventral longitudinal muscles and lateral muscles.

Our studies focus on the abdominal ventral muscles. These muscles form at the ventral midline, comprising clusters of 5–6 fibers in each central abdominal hemisegment (our data and (Bate et al., 1991; Broadie and Bate, 1991). In the embryo, a single ventral adult muscle precursor (AMP) is set aside in each abdominal hemisegment (Bate et al., 1991; Broadie and Bate, 1991; Figeac et al., 2010) (Fig. 1A). The proliferation of this precursor in larval life results in a cluster of about 8 myoblasts per abdominal hemisegment at the end of larval stages (Bate et al., 1991; Broadie and Bate, 1991). These myoblasts are closely associated with abdominal nerves (Bate et al., 1991; Dutta et al., 2004). In early pupal life, myoblast numbers increase, and the cells migrate out along the nerves. By 24h after puparium formation (APF) a small population of these cells begins to express high levels of the

founder cell (FC) marker *dumbfounded/Kirre (duf)* (Dutta et al., 2004). Each FC initiates the formation of a muscle fiber and fuses with additional myoblasts to form mature muscle fibers. Thus, FC number corresponds to the final fiber number.

The selection of FCs requires the Fibroblast Growth Factor (FGF) pathway (Dutta et al., 2005). This pathway is required for mesoderm spreading and differentiation in the embryo (Kadam et al., 2009). In early pupal life, the *heartless* FGF receptor (*htl*) is expressed in myoblasts. Expression of dominant negative *htl* decreases the number of founders, while increased expression of *htl* increases founder number and the number of lateral abdominal fibers. The source of the FGF ligands to activate *htl* has not been identified. In addition to *htl* in the FCs, the presence of the innervating motor neurons is also required for correct fiber number (Currie and Bate, 1995; Fernandes and Keshishian, 2005).

The genes *reaper* (*rpr*), *hid, grim* and *sickle* (*skl*) (the RHG genes) regulate the majority of somatic cell deaths in Drosophila (Grether et al., 1995; Kurada and White, 1998; Tan et al., 2011; Garcia-Hughes et al., 2015). We have described significant alterations in CNS cell death when *grim* and *rpr* are disrupted (Peterson et al., 2002; Tan et al., 2011; Arya et al., 2015). Neural stem cells or neuroblasts (NBs) that normally die in the central abdominal segments of the embryonic ventral nerve cord (VNC) survive inappropriately in *grim rpr* mutants. The surviving stem cells continue to divide, resulting in massive enlargement of the abdominal VNC. In the course of our characterization of RHG mutants, we also identified an alteration in the number of fibers in the ventral abdominal muscles. Here we show that inhibition of cell death in the nervous system can lead to increased ventral muscle FCs. A dramatic increase in ventral muscle innervation is detected, possibly due to the ectopic postembryonic birth of new motor neurons. We demonstrate that the increase in ventral muscle fiber number is due to the production of FGF ligands in the CNS. Finally, we show that cell death also intrinsically regulates founder cell number. We propose that motor neurons act as a source of FGF ligands to regulate founder cell number, at least in part by maintaining founder cell viability.

Results

In Drosophila, the RHG genes regulate developmental death in a tissue specific manner. The combinatorial expression of the RHG genes is controlled by tissue specific enhancers spread through the intergenic regions of the locus (Moon et al., 2005; Zhang et al., 2008; Tan et al., 2011; Arya et al., 2015). We identified a regulatory region between *grim* and *rpr* that specifically regulates the expression of *grim*, *rpr* and *skl* in the developing CNS (Tan et al., 2011).

In the course of these studies, we noted an adult muscle phenotype. The number of fibers in the ventral abdominal muscles was clearly increased in flies of the genotype *Df(3L)XR38/Df(3L)H99* (*XR38/H99*) or *Df(3L)XR38/(Df(3L)X20* (*XR38/X20*) (Fig. 1B–D). *XR38* deletes the *rpr* gene and approximately 50kb of the intergenic region between *rpr* and *grim* (Peterson et al., 2002). *H99* removes *hid*, *grim* and *rpr* and *X20* deletes *hid*, *grim*, *rpr* and *skl* (White et al., 1994; Tan et al., 2011). Our previous studies showed that the death of neural

stem cells in the developing embryo is profoundly inhibited in *XR38/H99* and *XR38/X20* animals (Peterson et al., 2002; Tan et al., 2011).

Inhibition of cell death leads to extra muscle fibers

To further analyze this phenotype, we quantified ventral muscle fiber numbers in a variety of genotypes using filet preparations of adult abdomens (Fig. 1E). In some preparations the VNC was retained to preserve innervating nerve fibers (Fig. 1F). We counted fiber numbers in ventral muscles in three mid-abdominal segments (A3-A5) from control and cell death defective animals. To differentiate individual fibers, we counted columns of nuclei, as they are aligned in an easily discernable column in each muscle fiber (Fig. 2A–E). In control animals, we observed the expected 10–12 fibers per segment (5–6/hemisegment) (Fig. 2A, 2F). To strongly inhibit rpr and grim dependent cell death, we used a *grim rpr* mutant ($grim^{C15E}$ rpr^{87} 3.5A/Df(3L)MM2) (3.5A/MM2) (Tan et al., 2011). In this mutant, the *grim* and *rpr* transcribed regions are deleted, as is one copy of the intergenic region. Ventral muscle fiber number was approximately doubled in these animals, indicating that cell death plays a role determining the number of ventral muscle fibers (Fig. 2D, 2F). We also noted an increased variability in muscle fiber number in the *grim rpr* mutants, with some muscles having as many as 27 fibers (Fig. 2F).

Cell death might limit the number of fusion competent myoblasts, while the absence of cell death could inhibit myoblast fusion (Hochreiter-Hufford et al., 2013). We counted the number of nuclei in each adult muscle fiber and found that there was no difference in the number of nuclei/ fiber, with wild type muscle fibers having an average of 12.4 2.7 ($x\bar{}$±SD) nuclei/fiber, while ventral fibers in the *grim rpr* mutants had an average of 12.5 ± 2.9 nuclei. These data indicate that myoblast fusion was not influenced in these cell death mutants, and suggests that cell death does not contribute to the process of myoblast fusion in these developing muscles.

We also detected a frequent abnormality in the patterning of muscle fibers in both the *grim rpr* mutants, and the heterozygotes that were missing one copy of *grim* and *rpr* (Fig. 2E). Rather than the standard longitudinal orientation of the fibers, we found some had formed a lateral “roof” across the midline (Fig. 2E’ arrow). We also observed persistent large larval nuclei at the midline of these abnormal segments (arrow in Fig. 2E’’). Delayed removal of larval nuclei, due to the decreased function of *grim* and *rpr*, may prevent the adult histoblasts from reaching the ventral midline. Muscle attachment sites present on the epidermis may therefore be mis-positioned in the mutant abdomens (Fernandes et al., 1996).

Cell death in the CNS limits fiber number

Our previous studies demonstrated a defect in NB death in the abdominal VNC in the *grim rpr* mutants (Peterson et al., 2002; Tan et al., 2011; Arya et al., 2015). We questioned whether the muscle phenotype we observed was a consequence of the lack of cell death in the developing CNS. To test this, we inhibited NB and neuronal apoptosis, using worniu-Gal4 (wor-Gal4) and elav-Gal4 to express the broad-spectrum caspase inhibitor p35. Wor-Gal4 drives strong expression in NBs starting at embryonic stage 11, and persists in NBs and their progeny through larval life (Arya et al., 2015). elav-Gal4 comes on slightly later in

embryonic neural development and is expressed weakly in some NBs and strongly in neurons into adulthood. When combined, elav-Gal4 and wor-Gal4 driving p35 apoptosis in NBs and neurons is inhibited from mid-embryonic stages into adult life.

We counted ventral muscle fibers in adults in *elav-Gal4*, *elav-Gal4 wor-Gal4* (*elav, wor-Gal4*), *elav-Gal4 UAS-p35* (*elav>p35*), *wor-Gal4 UAS-p35* (*wor>p35*) and *elav-Gal4 wor-Gal4 UAS-p35* (*elav, wor>p35*) (Fig. 3). We noted that elav-Gal4 alone had some effect on fiber number. Further addition of wor-Gal4 did not increase muscle fiber number (data not shown); therefore elav-Gal4 was used as a control (Fig. 3D). Fiber number was increased slightly, but not significantly in elav>p35 and wor>p35 (Fig. 3B, 3D). Another neuroblast/neuronal driver, inscute-Gal4, used to drive UAS-p35 had a similar effect on fiber number (data not shown). When combined, elav, wor> p35 had many more additional fibers (Fig. 3C, 3D). Thus, extra muscle fibers develop when cell death is inhibited in the embryonic NBs and their neuronal progeny.

In contrast, when we drove p35 with vGlut-Gal4, a driver expressed in motor neurons in the larvae and adult (Mahr and Aberle, 2006), fiber number was not altered (data not shown). These experiments indicate that blocking cell death in the mature motor neurons is not sufficient to increase fiber number.

We also counted the number of nuclei in each muscle fiber and found that this number was not changed significantly in elav, wor>p35 (13.3 ± 2.3 vs. 12.4 ± 2.7 in wild type). This indicates that the number of fusion competent myoblasts is not limiting, even when muscle fiber number is increased without inhibiting cell death in the myoblast pool.

Inhibition of death in the CNS results in increased ventrally projecting motor neurons

To further examine the relationship between innervation and increased muscle fiber number, we looked at preparations of adult abdomens in which the VNC had been retained (Fig. 1F). In the wild type, motor neuron branches enter the ventral muscles and innervate each fiber (Fig. 4A–B). In both the elav, wor>p35 animals, and the *grim rpr* mutants, the ventrally projecting motor axon tracts are much thicker, and the projections onto the ventral muscles are thicker and more exuberantly branched, suggesting that there might be more motor neurons projecting to these muscles (Fig. 4C–F).

Ventral muscle hyper-innervation could result from the prolonged survival of motor neurons born in the embryo. However, our data indicate that inhibiting cell death in both NBs and neurons results in the highest number of ectopic muscle fibers. This suggests that motor neurons born post-embryonically might project to ventral muscles causing increased fiber number. We tested whether we could detect motor neurons being born post-embryonically, by feeding larvae with BrdU throughout larval life and examining late third instar VNCs for BrdU incorporation in potential motor neurons.

Two markers were used that are expressed in ventrally projecting motor neurons. vGlut-Gal4 is an insertion that reports the expression of the vesicular glutamate transporter present in Drosophila motor neurons and some additional sensory neurons (Mahr and Aberle, 2006; Baek and Mann, 2009). The Hb9 homeodomain protein is another marker of motor neurons.

Some of the ventrally projecting motor neurons express Hb9 (Broihier and Skeath, 2002; Hebbar et al., 2006).

In control animals, many vGlut expressing neurons are visible in the abdominal neuromeres of the third instar larvae (Fig. 5A'). However, almost all of these are large neurons that are born embryonically. We did detect occasional abdominal neurons that were co-labeled with vGlut and BrdU in the control (not shown). These were always located in the ventral-lateral cluster. Very few thoracic neurons were co-labeled, despite the fact that leg motor neurons are born post-embryonically (Baek and Mann, 2009). This is likely due to the fact that vGlut is expressed relatively late in neuronal maturation (Mahr and Aberle, 2006), and thus is not yet expressed in the newly born post-embryonic motor neurons.

In the *grim rpr* mutant, we were able to detect an increased number of double-labeled cells in the abdominal VNC (Fig. 5B–C). These small cells expressed low levels of vGlut and were located in both the ventral lateral and medial region of the abdominal VNC. Thus, inhibition of cell death results in increased numbers of glutamatergic neurons. However, we concluded that this experiment was likely to underestimate the number of glutamatergic neurons born in the *grim rpr* nervous system, due to the low levels of vGlut expression in the newly born adult motor neurons in the larvae.

In wild type larvae, Hb9 marks three pairs of thoracic lineages of leg motor neurons. These clustered thoracic lineages consist of both embryonically and post-embryonically born neurons (Lacin et al., 2014) (Fig. 5D–D'). In wild type larvae, there are few Hb9 positive neurons in the abdominal segments of the VNC. These consist of embryonically born motor neurons and some interneurons (Banerjee, Toral, Conway, Siefert, Dorr and Fernandes, personal communication). Our data confirm that no Hb9 expressing neurons are born post-embryonically in the abdominal neuromeres of wild type larvae, as no co-labeling of BrdU was seen with Hb9 (not shown).

In *grim rpr* mutant larvae, we found a great increase in Hb9 positive cells in the abdominal segments (Fig. 5E–H). These ectopic Hb9 positive cells were in medially located clusters, reminiscent of the thoracic clusters of Hb9 positive cells, albeit smaller. Many of these cells were double labeled with BrdU (Fig. 5F). This suggests that the NBs that normally give rise to the leg motor neurons in the thoracic regions are rescued from death in the abdominal segments of the *grim rpr* mutants, and proliferate to ectopically produce Hb9 positive neurons.

Post-embryonically born Hb9 cells were organized in clusters of small cells (Fig.5F, G). We also detected an increase in embryonically born (non BrdU) Hb9 positive cells in the *grim rpr* mutant VNCs (Fig. 5H). Previous studies have demonstrated an increase in Hb9 expressing cells in cell death defective embryos (Rogulja-Ortmann et al., 2007). These cells are retained in the *grim rpr* mutant VNCs.

To further examine the contribution of Hb9 expressing neurons to ventral abdominal muscle innervation, we examined filet preps from wild type and *grim rpr* mutant animals with Hb9-Gal4 UAS-mCD8-GFP (Broihier and Skeath, 2002; Hebbar et al., 2006). By co-labeling with the neuronal marker 22C10, we found that the ventral muscles in segment A2 are

robustly innervated by Hb9-Gal4 expressing neurons, as previously reported (Fig. 5I) (Hebbar et al., 2006). However, in segment A3 Hb9-Gal4 expressing neurons make a much smaller contribution to the ventral muscle innervation (Fig. 5J). In the *grim rpr* mutant, Hb9-Gal4 expressing cells are still only minor contributors, despite a large increase in innervation, as visualized with 22C10 (Fig. 5K). We conclude that other lineages of motor neurons are increased in the absence of cell death.

These experiments indicate that increased innervation of ventral muscles is likely to arise from ectopic motor neurons, of both embryonic and postembryonic origins. Taken together with the elav, wor>p35 experiments shown in Fig. 3, and the lack of an effect of vGlut>p35, these data suggest that muscle fiber number is most increased when both embryonic motor neuron and post-embryonic NBs that generate additional motor neurons are protected from death.

Inhibition of cell death in the CNS results in extra founder cells

In normal adult abdominal muscle development, each fiber is pioneered by a single founder cell (FC) (Dutta et al., 2004). FCs express high levels of Duf on their surface starting at about 24 hours APF for abdominal muscles. By 50 hours APF, fusion-competent myoblasts also express low levels of Duf, but the single FC nucleus in each fiber still expresses a higher level of Duf. To determine whether inhibition of cell death in the CNS resulted in extra FCs, we examined duf-lacZ expression in pupae. In both the *grim rpr* mutant and in wor>p35, we detect increased numbers of duf-lacZ positive FCs (Fig. 6). This indicates that inhibition of cell death in the CNS increases the number of FCs specified in pupal development.

FGFs in the CNS contribute to extra muscle fibers in cell death mutants

The experiments above demonstrate that ectopic survival of cells in the CNS, most likely including ventrally targeted motor neurons, results in increased numbers of FCs, and consequently increased ventral fiber numbers. This suggests that a signal from the nerves impacts founder cell number.

Fibroblast Growth Factors (FGFs) are a candidate for this signal. The FGF receptor *htl* is involved in many aspects of muscle development. Most pertinently, *htl* in the myoblasts is required for upregulation of *duf* in adult FCs, and ectopic *htl* expression in myoblasts results in increased founder and fiber numbers in the lateral fibers of the adult abdomen (Dutta et al., 2005). Although there has been some previous suggestion that the FGF ligands may not be limiting in the wild type situation (Dutta et al., 2005), we hypothesized that increased motor neurons in the cell death mutants might be a source of increased FGF ligands, leading to increased *htl* activity.

The *htl* ligands, *pyramus* (*pyr*) and *thisbe* (*ths*), are expressed in the early embryo (Kadam et al., 2009). These ligands have overlapping but distinct activities in mesoderm spreading. In addition, they are expressed in the developing CNS and are involved in glial migration and synaptogenesis (Sen et al., 2011; Stork et al., 2014). To test whether these ligands are required in the CNS for the increased ventral fiber formation, we used RNAi constructs to knock down the ligands in the CNS, while at the same time blocking NB and neuronal cell death with p35. We found that knocking down *ths* significantly decreased the number of

ectopic ventral muscle fibers, while pyr-RNAi had a smaller effect (Fig. 7A). Furthermore, animals heterozygous for a deletion that removes both ligands reduces the ventral muscle fiber number to that of control (Fig. 7A).

Hyper-innervation was still evident in the ventral muscles of the elav, wor>p35 ths-RNAi adults (Fig. 7B), suggesting that FGF knockdown does not influence motor neuron survival. In fact, in the elav, wor>p35 ths-RNAi ventral abdominal muscles we noted an increase in incoming axons that did not seem to connect with muscle targets (arrows in Fig. 7B', C). We propose that excess motor neuron survival results in an increase of *pyr* and *ths*. These ligands then function in a partially redundant manner to increase the number of FCs, and thus fiber number. We could not test the effects of overexpressing the ligands on adult muscle, as CNS expression of the ligands results in lethality.

Intrinsic role for cell death in myoblasts

Inhibition of cell death in the developing CNS with elav, wor>p35 increases ventral muscle fiber number substantially, but not to the same extent as in the mutants that remove *grim* and *rpr*. We wondered whether founder cell survival might also play a role in determining the final number of founders in the adult ventral muscles. In the development of the caudal visceral mesoderm, *pyr* and *ths* not only function as guidance signals, but also promote the survival of muscle founders (Reim et al., 2012). To test for an intrinsic role for cell death in myoblasts, we inhibited cell death in *duf* expressing cells with p35. As duf is expressed in the embryo and in the adult FCs, we used Gal80^{ts} to limit expression of p35 to embryonic and larval stages, or to pupal and adult stages (Fig. 8A).

When p35 was expressed in *duf* expressing cells only in the embryo and larvae, we saw approximately the same number of fibers as in control animals exposed to the same temperature regimen (Fig. 8B). This indicates that cell death in embryonic and larval stages does not play a major role in determining the number of ventral muscle fibers in the adult. This finding agrees with previous work showing ventral AMPs in the embryo are not influenced by cell death (Figeac et al., 2010).

When p35 was expressed in *duf* expressing cells in pupal and adult stages, fiber number increased significantly compared to control (Fig. 8B). We conclude that cell death plays two roles in muscle development. It limits the number of motor neurons projecting to the ventral muscles, and it limits the number of FCs specified during pupal life. To test this further, we examined fiber number in animals expressing p35 in NBs, neurons and myogenic cells using elav-Gal4, wor-Gal4 and duf-Gal4 together to express p35. We saw a significant increase in fiber number over control, although the mean number of fibers was not increased over elav, wor> p35 (Fig. 8C, 8D). However, we saw a large animal to animal variation in fiber number, with some animals having a very large increase in fiber number, similar to what we saw in the *grim rpr* mutant (Fig. 8C, 8D).

Discussion

An important role of cell death during development is to coordinate cell numbers in interacting tissues (Fuchs and Steller, 2011; Arya and White, 2015). The balance between

proliferation and death in both tissues allows for plasticity in the face of differing environmental and genetic cues. Both anterograde and retrograde trophic interactions may play a role in regulating this balance. In this work, we have examined how cell death influences muscle development, exploring cell death both in the mesoderm and in the interacting nervous system.

Interactions between motor neurons and muscle precursors coordinate adult muscle development in the fly (Currie and Bate, 1995; Fernandes and Keshishian, 2005; Dutta et al., 2010). Here we show that the regulation of cell death is an important component of that interaction. Cell death limits the number of motor neurons that target the ventral abdominal muscles of the fly. Our data suggest that if excess motor neurons are allowed to survive, they will produce increased levels of FGFs, which promote the specification and survival of additional FCs, leading to increased numbers of muscle fibers. Thus, cell death regulates muscle fiber numbers both non-autonomously through the CNS, and autonomously in the myoblasts.

There are interesting parallels between our findings and previous work in mammalian model systems. Studies on the role of innervation in muscle development in vertebrates show that formation of myotubes, particularly secondary myotubes, is decreased in the absence of innervation (Wilson and Harris, 1993). Pertinent to our work, the presence of increased motor neurons in the muscular dysgenesis (mdg) mouse mutant results in a doubling of the number of secondary fibers in limb muscles (Oppenheim et al., 1986; Ashby et al., 1993). Thus, anterograde factors can regulate myotube number in both flies and mammals.

When motor neuron death is limited, we find that FGFs are required in the developing CNS to cause increased muscle fiber number. Although the most parsimonious explanation for this finding is that increased FGF in the ectopic motor-neurons acts directly on the myoblasts to increase FC number through activation of the *htl* receptor, we cannot rule out an indirect role for *pyr* and *ths* in fiber survival, perhaps through synaptic contact (Sen et al., 2011; Nonomura et al., 2013). We therefore conclude that cell death in the CNS normally limits the level of FGFs produced, directly or indirectly limiting fiber number. Interestingly, in mammalian brain development, cell death is required to limit the production of FGF8 to allow proper forebrain development (Nonomura et al., 2013).

Our data also indicate that cell death is important in the myoblast population to limit FC and fiber number. FGF signaling could promote FC viability. Alternatively, there may be myoblast intrinsic signaling that limits muscle fiber cell number, similar to myostatin in mammalian muscle development (Lee, 2004).

This study illustrates how defects in the proper regulation of cell death can disrupt the developmentally important interactions between the CNS and its target tissues. Given that the focus of most developmental cell death is in the CNS, it is likely that additional important interactions may be uncovered with further study of these cell death mutants.

Materials and methods

Fly strains

The following RHG region deletions were used in this study: Df(3L)XR38 (XR38), which deletes the intragenic regulatory region between *grim* and *rpr*, as well the *rpr* and *skl* coding regions (Peterson et al., 2002), Df(3L)H99 (H99), which deletes from *hid* through *rpr* (White et al., 1994), Df(3L)X20 (X20), which deletes from *hid* through *skl* (Tan et al., 2011), and Df(3L)MM2 (MM2) which deletes about 110 kb from *grim* through *rpr* (Tan et al., 2011). The *grim rpr* mutation (3.5A) is a recombinant of a small *rpr* deletion (rpr^{87}) and $grim^{C15E}$ (Wu et al., 2010; Tan et al., 2011). worniu (wor)-Gal4 (Albertson et al., 2004) and C155 (elav)-Gal4 (Lin and Goodman, 1994) (Bloomington stock center) were used to drive expression of UAS-p35 (Hay et al., 1994) in the developing CNS. rp298 -lacZ and rp298 -Gal4 lines were both obtained from Mary Baylies. They are enhancer trap P-element insertions in the *duf* gene (Ruiz-Gomez et al., 2000). $vGlut^{ok371}$-Gal4 (Mahr and Aberle, 2006) was used to drive expression of nuclear localized dsRED (Bloomington Stock Center) to visualize glutamatergic neurons. Hb9-Gal4 (Bloomington stock center) was used to drive GFP expression in subsets of motorneurons (Hebbar et al., 2006). Hb9-Gal4 was recombined with the MM2 deletion to drive GFP in *grim rpr* mutants (3.5A/MM2). UAS-thisbe-RNAi (ths RNAi) and UAS-pyramus-RNAi (pyr RNAi) (Vienna Drosophila Research Center) and Df(2R)BSC25 (Bloomington Stock Center) were used to inhibit FGF signaling. Temperature sensitive Gal80 (Bloomington Stock Center) was used to repress the expression of rp298 -Gal4 and hence the expression UAS-p35 at 18°C.

Filet preparation

All flies were raised at 25°C unless otherwise stated. Abdomens from flies no more than 4 days old were dissected away from the rest of the animal. Using fine surgical scissors, abdomens were cut along the dorsal midline, viscera were removed and the filet was pinned flat on a Sylgard dish. For preparations where CNS as left intact, whole abdomens were pinned and incisions were made along the dorsal midline through the abdomen and thorax. After pinning, filet preparations were fixed in 4% paraformaldehyde in phosphate buffered saline (PBS) for 30 minutes, and washed with PBS-Triton-X (0.3%) and processed for immunohistochemistry.

Pupal preparations were done similar to adult preparations. White pre-pupae (0 ± 1h APF) were collected and aged for 44 hours at 25°C (44h APF). Pupal muscle dissections were preformed as described previously (Morriss et al., 2012). Cutting along the dorsal midline allowed the visualization of the abdominally developing ventral muscles.

CNS preparations and BrdU treatment

5-bromodeoxyuridine (BrdU) incorporation was done by growing larvae on food with 0.1mg/ml BrdU (White and Kankel, 1978). The CNS of late wondering third instar larvae was dissected in PBS, fixed in 2% paraformaldehyde in PBS-TritonX (0.3%) for 15 minutes, and washed with PBS-Triton-X (0.3%). Samples were washed once with 1X DNase I reaction buffer and then incubated in 0.2U/ul of DNase I (New England BioLabs) at 37°C

for one hour. After incubation in DNase I, the CNS were washed in PBS-Triton-X (0.3%) and processed for immunohistochemistry.

Immunohistochemistry

All preparations were blocked in 5–10% normal goat serum in PBS-Triton X (0.3%). Adult muscles were visualized with Rhodamine phalloidin (1:1000 Invitrogen) and muscle nuclei with Hoechst 33342 (1:1000 Molecular Probes). The following antibodies were used: anti-β-galactosidase (rabbit 1:1000 MP Biomedicals), anti-22C10 (mouse 1:5000 Developmental Studies Hybridoma Bank), anti-MHC antibody and Anti-BrdU antibody (rat 1:2000 Abcam). Anti-Hb9 antibody, a gift from James Skeath (Washington University School of Medicine, Saint Louis, MO), was used at a dilution of 1:2000. All primary antibody staining was done overnight at 4°C. Secondary antibody staining was done either overnight at 4°C or at least 2hours at room temperature. Stainings were visualized with a Nikon A1 confocal, and images were processed in Nikon Elements and Photoshop.

Quantifications and Data Analysis

Fiber numbers for each segment were counted based on DNA staining of multinucleate fibers. An aligned string of nuclei was counted as an individual fiber. Three segments (A3, A4, A5) per abdomen were counted for all genotypes.

All graphs and statistical analysis were done using GraphPad Prism7 software.

Acknowledgments

We would like to thank Mary Baylies, the VDRC and the Bloomington Stock Center for important fly stocks, the Developmental Studies Hybridoma Bank, Rachel Wilson and Jim Skeath for antibodies, and the CBRC confocal core. Joyce Fernandes shared important unpublished data and advice. The work was supported by grants GM56920 to BJT and GM110477 and S10RR027673 to KW.

Refs

Albertson R, Chabu C, Sheehan A, Doe CQ. Scribble protein domain mapping reveals a multistep localization mechanism and domains necessary for establishing cortical polarity. J Cell Sci. 2004; 117:6061–6070. [PubMed: 15536119]

Arya R, Sarkissian T, Tan Y, White K. Neural stem cell progeny regulate stem cell death in a Notch and Hox dependent manner. Cell Death Differ. 2015; 22:1378–1387. [PubMed: 25633198]

Arya R, White K. Cell death in development: Signaling pathways and core mechanisms. Semin Cell Dev Biol. 2015; 39:12–19. [PubMed: 25668151]

Ashby PR, Pincon-Raymond M, Harris AJ. Regulation of myogenesis in paralyzed muscles in the mouse mutants peroneal muscular atrophy and muscular dysgenesis. Dev Biol. 1993; 156:529–536. [PubMed: 8462749]

Atreya KB, Fernandes JJ. Founder cells regulate fiber number but not fiber formation during adult myogenesis in Drosophila. Dev Biol. 2008; 321:123–140. [PubMed: 18616937]

Baek M, Mann RS. Lineage and birth date specify motor neuron targeting and dendritic architecture in adult Drosophila. J Neurosci. 2009; 29:6904–6916. [PubMed: 19474317]

Bate M. The embryonic development of larval muscles in Drosophila. Development. 1990; 110:791–804. [PubMed: 2100994]

Bate M, Rushton E, Currie DA. Cells with persistent twist expression are the embryonic precursors of adult muscles in Drosophila. Development. 1991; 113:79–89. [PubMed: 1765010]

Broadie KS, Bate M. The development of adult muscles in Drosophila: ablation of identified muscle precursor cells. Development. 1991; 113:103–118. [PubMed: 1764988]

Broihier HT, Skeath JB. Drosophila homeodomain protein dHb9 directs neuronal fate via crossrepressive and cell-nonautonomous mechanisms. Neuron. 2002; 35:39–50. [PubMed: 12123607]

Currie DA, Bate M. Innervation is essential for the development and differentiation of a sex-specific adult muscle in Drosophila melanogaster. Development. 1995; 121:2549–2557. [PubMed: 7671818]

Dutta D, Anant S, Ruiz-Gomez M, Bate M, VijayRaghavan K. Founder myoblasts and fibre number during adult myogenesis in Drosophila. Development. 2004; 131:3761–3772. [PubMed: 15262890]

Dutta D, Shaw S, Maqbool T, Pandya H, Vijayraghavan K. Drosophila Heartless acts with Heartbroken/Dof in muscle founder differentiation. PLoS Biol. 2005; 3:e337. [PubMed: 16207075]

Dutta D, Umashankar M, Lewis EB, Rodrigues V, Vijayraghavan K. Hox genes regulate muscle founder cell pattern autonomously and regulate morphogenesis through motor neurons. J Neurogenet. 2010; 24:95–108. [PubMed: 20615088]

Fernandes JJ, Celniker SE, VijayRaghavan K. Development of the indirect flight muscle attachment sites in Drosophila: role of the PS integrins and the stripe gene. Dev Biol. 1996; 176:166–184. [PubMed: 8660859]

Fernandes JJ, Keshishian H. Motoneurons regulate myoblast proliferation and patterning in Drosophila. Dev Biol. 2005; 277:493–505. [PubMed: 15617689]

Figeac N, Jagla T, Aradhya R, Da Ponte JP, Jagla K. Drosophila adult muscle precursors form a network of interconnected cells and are specified by the rhomboid-triggered EGF pathway. Development. 2010; 137:1965–1973. [PubMed: 20463031]

Fuchs Y, Steller H. Programmed cell death in animal development and disease. Cell. 2011; 147:742–758. [PubMed: 22078876]

Garcia-Hughes G, Link N, Ghosh AB, Abrams JM. Hid arbitrates collective cell death in the Drosophila wing. Mech Dev. 2015

Grether ME, Abrams JM, Agapite J, White K, Steller H. The *head involution defective* gene of *Drosophila melanogaster* functions in programmed cell death. Genes Dev. 1995; 9:1694–1708. [PubMed: 7622034]

Hay BA, Wolff T, Rubin GM. Expression of baculovirus P35 prevents cell death in Drosophila. Development. 1994; 120:2121–2129. [PubMed: 7925015]

Hebbar S, Hall RE, Demski SA, Subramanian A, Fernandes JJ. The adult abdominal neuromuscular junction of Drosophila: a model for synaptic plasticity. J Neurobiol. 2006; 66:1140–1155. [PubMed: 16838368]

Hochreiter-Hufford AE, Lee CS, Kinchen JM, Sokolowski JD, Arandjelovic S, Call JA, Klibanov AL, Yan Z, Mandell JW, Ravichandran KS. Phosphatidylserine receptor BAI1 and apoptotic cells as new promoters of myoblast fusion. Nature. 2013; 497:263–267. [PubMed: 23615608]

Kadam S, McMahon A, Tzou P, Stathopoulos A. FGF ligands in Drosophila have distinct activities required to support cell migration and differentiation. Development. 2009; 136:739–747. [PubMed: 19158183]

Kurada P, White K. Ras promotes cell survival in *Drosophila* by downregulating *hid* expression. Cell. 1998; 95:319–329. [PubMed: 9814703]

Lacin H, Zhu Y, Wilson BA, Skeath JB. Transcription factor expression uniquely identifies most postembryonic neuronal lineages in the Drosophila thoracic central nervous system. Development. 2014; 141:1011–1021. [PubMed: 24550109]

Lee SJ. Regulation of muscle mass by myostatin. Annu Rev Cell Dev Biol. 2004; 20:61–86. [PubMed: 15473835]

Lin DM, Goodman CS. Ectopic and increased expression of Fasciclin II alters motoneuron growth cone guidance. Neuron. 1994; 13:507–523. [PubMed: 7917288]

Mahr A, Aberle H. The expression pattern of the Drosophila vesicular glutamate transporter: a marker protein for motoneurons and glutamatergic centers in the brain. Gene Expr Patterns. 2006; 6:299–309. [PubMed: 16378756]

Moon NS, Frolov MV, Kwon EJ, Di Stefano L, Dimova DK, Morris EJ, Taylor-Harding B, White K, Dyson NJ. Drosophila E2F1 has context-specific pro- and antiapoptotic properties during development. Dev Cell. 2005; 9:463–475. [PubMed: 16198289]

Morriss GR, Bryantsev AL, Chechenova M, LaBeau EM, Lovato TL, Ryan KM, Cripps RM. Analysis of skeletal muscle development in Drosophila. Methods Mol Biol. 2012; 798:127–152. [PubMed: 22130835]

Nonomura K, Yamaguchi Y, Hamachi M, Koike M, Uchiyama Y, Nakazato K, Mochizuki A, Sakaue-Sawano A, Miyawaki A, Yoshida H, Kuida K, Miura M. Local apoptosis modulates early mammalian brain development through the elimination of morphogen-producing cells. Developmental cell. 2013; 27:621–634. [PubMed: 24369835]

Oppenheim RW, Houenou L, Pincon-Raymond M, Powell JA, Rieger F, Standish LJ. The development of motoneurons in the embryonic spinal cord of the mouse mutant, muscular dysgenesis (mdg/mdg): survival, morphology, and biochemical differentiation. Dev Biol. 1986; 114:426–436. [PubMed: 3956874]

Peterson C, Carney GE, Taylor BJ, White K. reaper is required for neuroblast apoptosis during Drosophila development. Development. 2002; 129:1467–1476. [PubMed: 11880355]

Piccirillo R, Demontis F, Perrimon N, Goldberg AL. Mechanisms of muscle growth and atrophy in mammals and Drosophila. Dev Dyn. 2014; 243:201–215. [PubMed: 24038488]

Reim I, Hollfelder D, Ismat A, Frasch M. The FGF8-related signals Pyramus and Thisbe promote pathfinding, substrate adhesion, and survival of migrating longitudinal gut muscle founder cells. Dev Biol. 2012; 368:28–43. [PubMed: 22609944]

Rogulja-Ortmann A, Luer K, Seibert J, Rickert C, Technau GM. Programmed cell death in the embryonic central nervous system of Drosophila melanogaster. Development. 2007; 134:105–116. [PubMed: 17164416]

Ruiz-Gomez M, Coutts N, Price A, Taylor MV, Bate M. Drosophila dumbfounded: a myoblast attractant essential for fusion. Cell. 2000; 102:189–198. [PubMed: 10943839]

Schejter ED, Baylies MK. Born to run: creating the muscle fiber. Curr Opin Cell Biol. 2010; 22:566–574. [PubMed: 20817426]

Sen A, Yokokura T, Kankel MW, Dimlich DN, Manent J, Sanyal S, Artavanis-Tsakonas S. Modeling spinal muscular atrophy in Drosophila links Smn to FGF signaling. J Cell Biol. 2011; 192:481–495. [PubMed: 21300852]

Stork T, Sheehan A, Tasdemir-Yilmaz OE, Freeman MR. Neuron-glia interactions through the Heartless FGF receptor signaling pathway mediate morphogenesis of Drosophila astrocytes. Neuron. 2014; 83:388–403. [PubMed: 25033182]

Tan Y, Yamada-Mabuchi M, Arya R, St Pierre S, Tang W, Tosa M, Brachmann C, White K. Coordinated expression of cell death genes regulates neuroblast apoptosis. Development. 2011; 138:2197–2206. [PubMed: 21558369]

White K, Grether ME, Abrams JM, Young L, Farrell K, Steller H. Genetic control of programmed cell death in *Drosophila*. Science. 1994; 264:677–683. [PubMed: 8171319]

White K, Kankel DR. Patterns of cell division and cell movement in the formation of the imaginal nervous system in Drosophila melanogaster. Dev Biol. 1978; 65:296–321. [PubMed: 98369]

Wilson SJ, Harris AJ. Formation of myotubes in aneural rat muscles. Dev Biol. 1993; 156:509–518. [PubMed: 8462747]

Wu JN, Nguyen N, Aghazarian M, Tan Y, Sevrioukov EA, Mabuchi M, Tang W, Monserrate JP, White K, Brachmann CB. grim promotes programmed cell death of Drosophila microchaete glial cells. Mech Dev. 2010

Zhang Y, Lin N, Carroll PM, Chan G, Guan B, Xiao H, Yao B, Wu SS, Zhou L. Epigenetic blocking of an enhancer region controls irradiation-induced proapoptotic gene expression in Drosophila embryos. Dev Cell. 2008; 14:481–493. [PubMed: 18410726]

Highlights

- Cell death mutants have increased fibers in the adult ventral abdominal muscles
- Inhibition of cell death in the nervous system increases muscle fiber number
- Increased muscle fiber number requires FGFs in the nervous system
- Autonomous cell death in the myoblast lineage also limits muscle fiber number

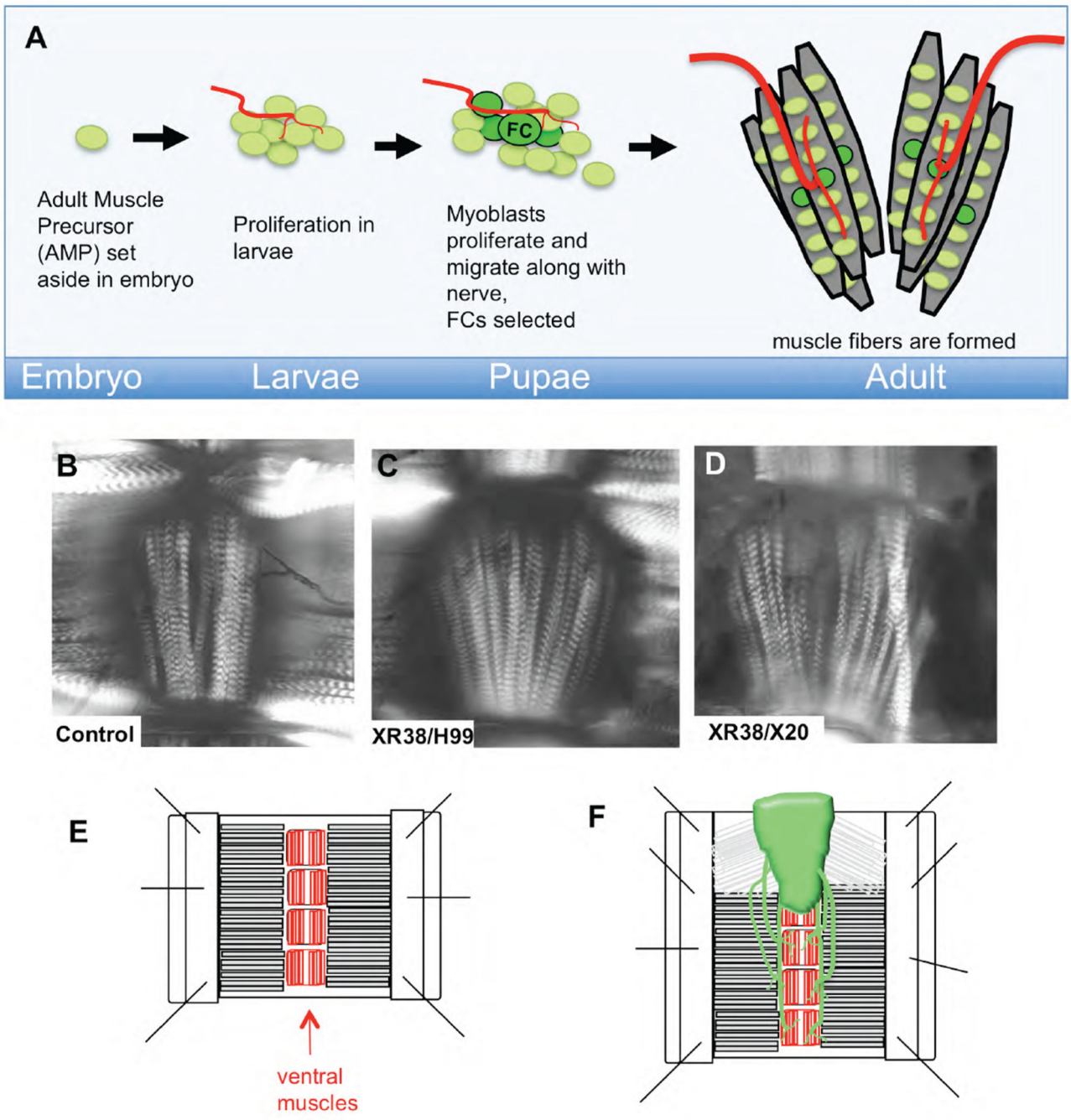

Figure 1. Cell death mutants have increased fibers in abdominal ventral muscles

A) In the early embryo, a small number of adult muscle precursors (AMPs) are born from muscle progenitors, but remain quiescent until larval life, when they begin to proliferate (Figeac et al., 2010). In pupal life, these myoblasts proliferate further and migrate along nerves towards their eventual locations. Founder Cell (FC) selection takes place in the abdomen starting at 24h APF (Dutta et al., 2004). Fusion competent myoblasts then fuse with the FCs to form muscle fibers.

B–D) Ventral abdominal muscles from young females were examined by polarized light (shown as focal plane composites). Increased muscle fiber number is readily obvious in, XR38/H99 (**C**) and XR38/X20 (**D**) cell death defective adults compared to control **(B). E, F)** Diagram of adult abdomen filet preparations used to visualize muscles. Abdomens were opened at the dorsal midline, pinned, fixed and stained. Ventral nerve cords (VNCs) were retained in some preps (**F**).

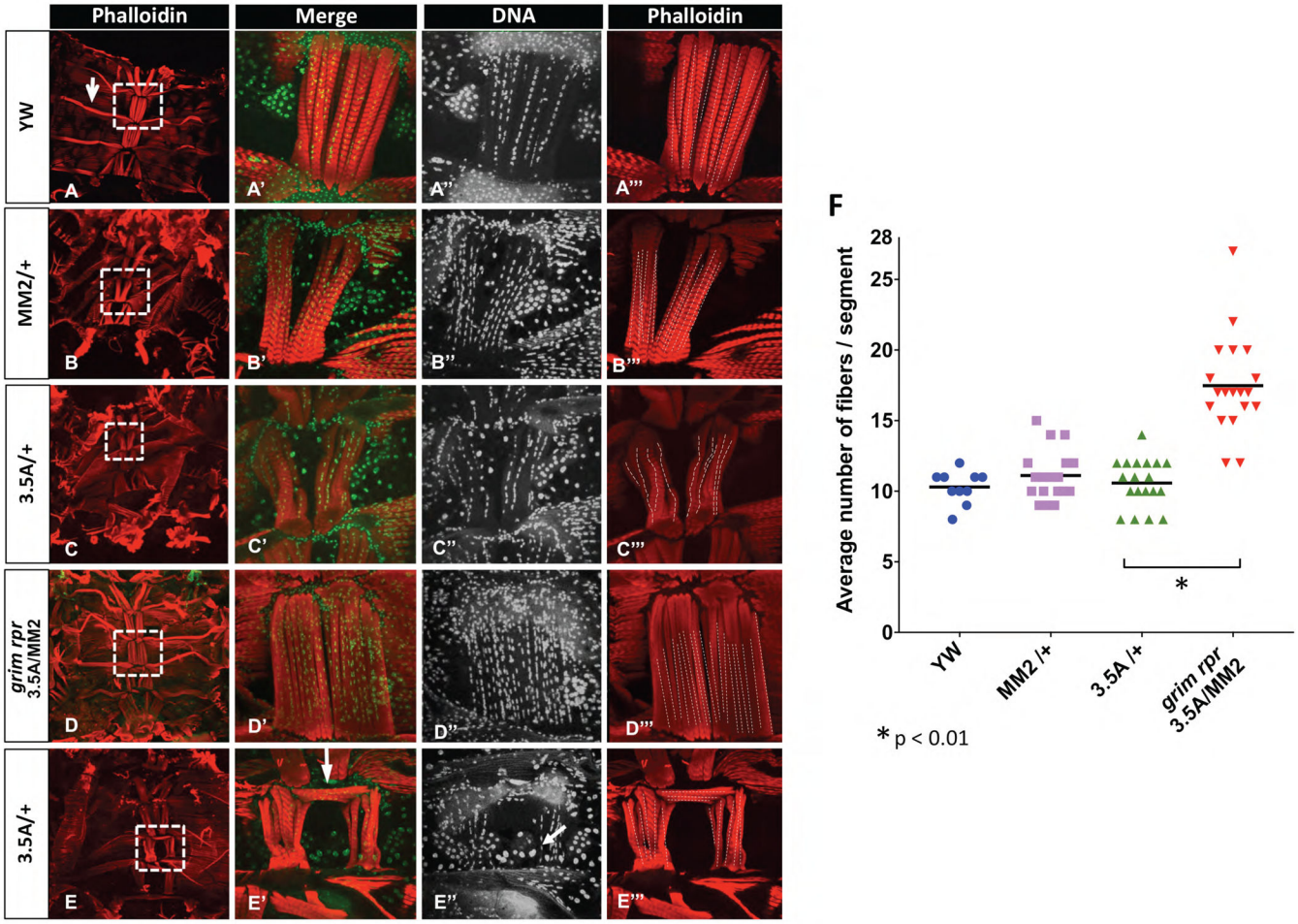

Figure 2. In the absence of *grim* and *rpr* ventral muscle fiber number is doubled

A–E”’) Abdominal filet preps stained with phalloidin (red) to mark muscles, and Hoechst 33342 (green) to mark DNA. Fiber numbers were quantified by counting columns of nuclei, as shown in **A”-E”**, and illustrated with dashed lines in **A”’-E”’**. Heterozygotes for the *grim rpr* double mutant (3.5A) and the *grim* to *rpr* deletion (MM2) have an average of 10 fibers/segment. When *grim* and *rpr* are completely removed in 3.5A/MM2, fiber number is dramatically increased to about 15–20 fibers/segment (**D–D”’, F**). Adults were dissected within 2 days of eclosion, and many retain distinctive larval muscles (**arrow in A**). In both heterozygous and homozygous *grim rpr* mutants we frequently noted transverse ventral muscle fibers (**arrow in E’**), possibly due to the retention of large larval epidermal cells at the ventral midline (**arrow in E”**). **F**) Quantification of average number of fibers per segment. Three segments per abdomen (A3-A5) were counted ($\bar{x}$ shown as bar.) Animals/genotype yw n=5, MM2/+ n=8, 3.5A/+ n=8, 3.5A/MM2 n=10. Images were either taken at a magnification of 10X **(A–E)** or 60X **(A’-B’)**.

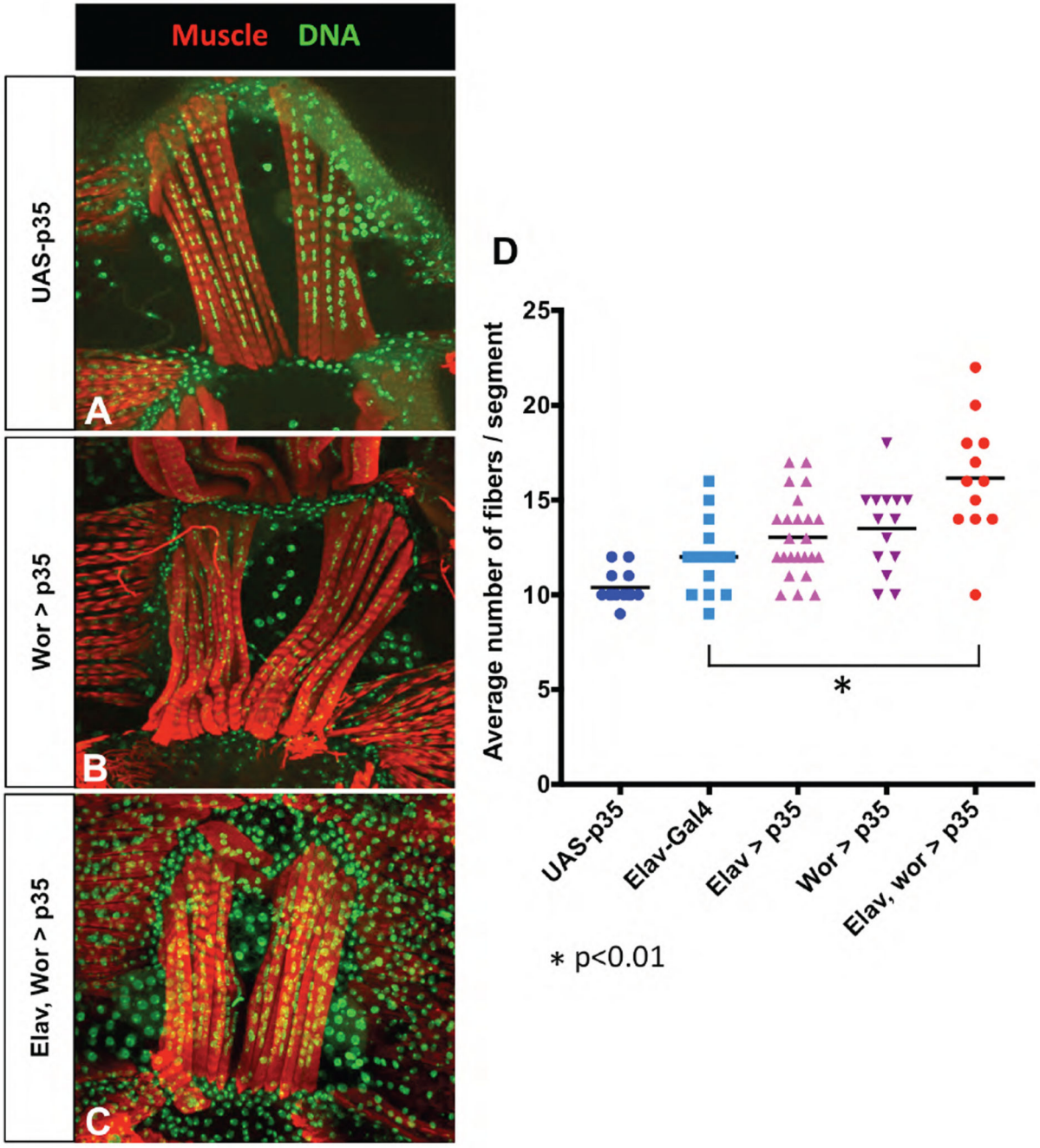

Figure 3. Inhibition of cell death in the CNS results in increased ventral muscle fibers

The broad-spectrum caspase inhibitor p35 was used to inhibit cell death exclusively in the developing CNS. **A)** UAS-p35 alone had wild type fiber numbers **B**) expression of p35 with wor-Gal4 rescues embryonic abdominal NBs, and increases muscle fiber numbers. **C**) Combining wor-Gal4 with elav-Gal4 rescues both NBs and neurons, and results in a significant increase in fiber number. **D)** Fiber number counts ($\bar{x}$ shown as bar). elav-Gal4 alone results in an increase in fiber number, but both elav>p35 and wor>35 increased fiber number slightly more, and when combined the two drivers together showed a significant

increase (* $p<0.05$ vs. elav-Gal4, wor-Gal4). Animals/genotype UAS-p35 n=7, elav-Gal4 wor-Gal4 n=4, elav>p35 n=8, wor>p35 n=7, elav wor>p35 n=4.

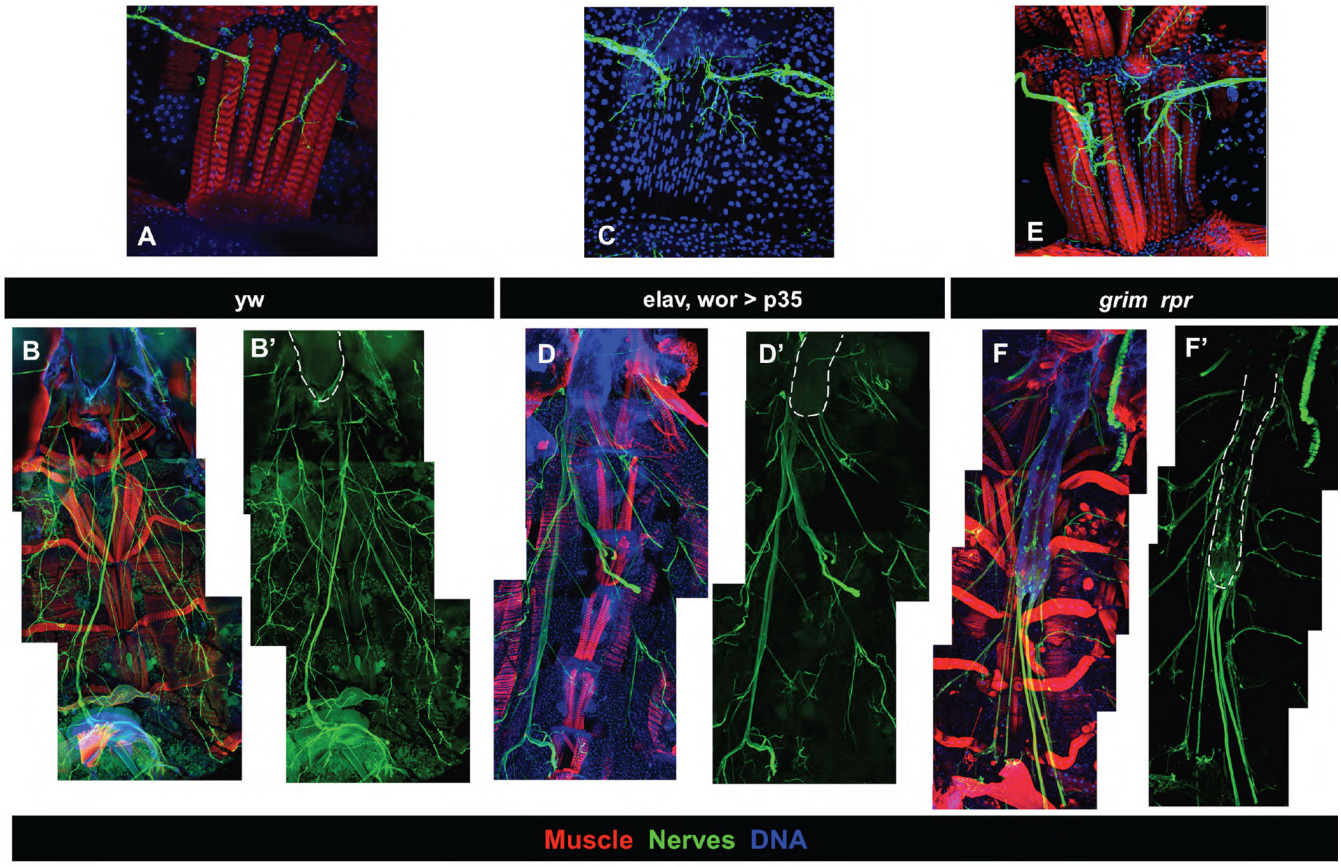

Figure 4. Ventral muscles are hyper-innervated in cell death mutants

Filet preps of young adults with the VNC included were used to examine ventral muscle innervation in wild type (**A, B**), elav, wor>p35 (**C, D**), and the *grim rpr* mutant (3.5A/MM2) (**E, F**). Muscles are stained with phalloidin (red)(except in **C**), DNA with Hoechst 33342 (blue), and nerves with 22C10 (**A–E**) or with elav-Gal4 mCD8-GFP (**F**). **A, C, E**) 60X images of a single abdominal segment showing ventral muscle innervation. Inhibition of cell death in the CNS (**C–D**) or the whole animal (**E–F**) results in a thickened incoming axon tract and extensive branching. **B,D,F**) 20X images stitched together to show abdominal VNC (outlined in white) relative to muscles. elav, wor>p35 results in a slight extension of the VNC, while the *grim rpr* mutant has a very extended VNC.

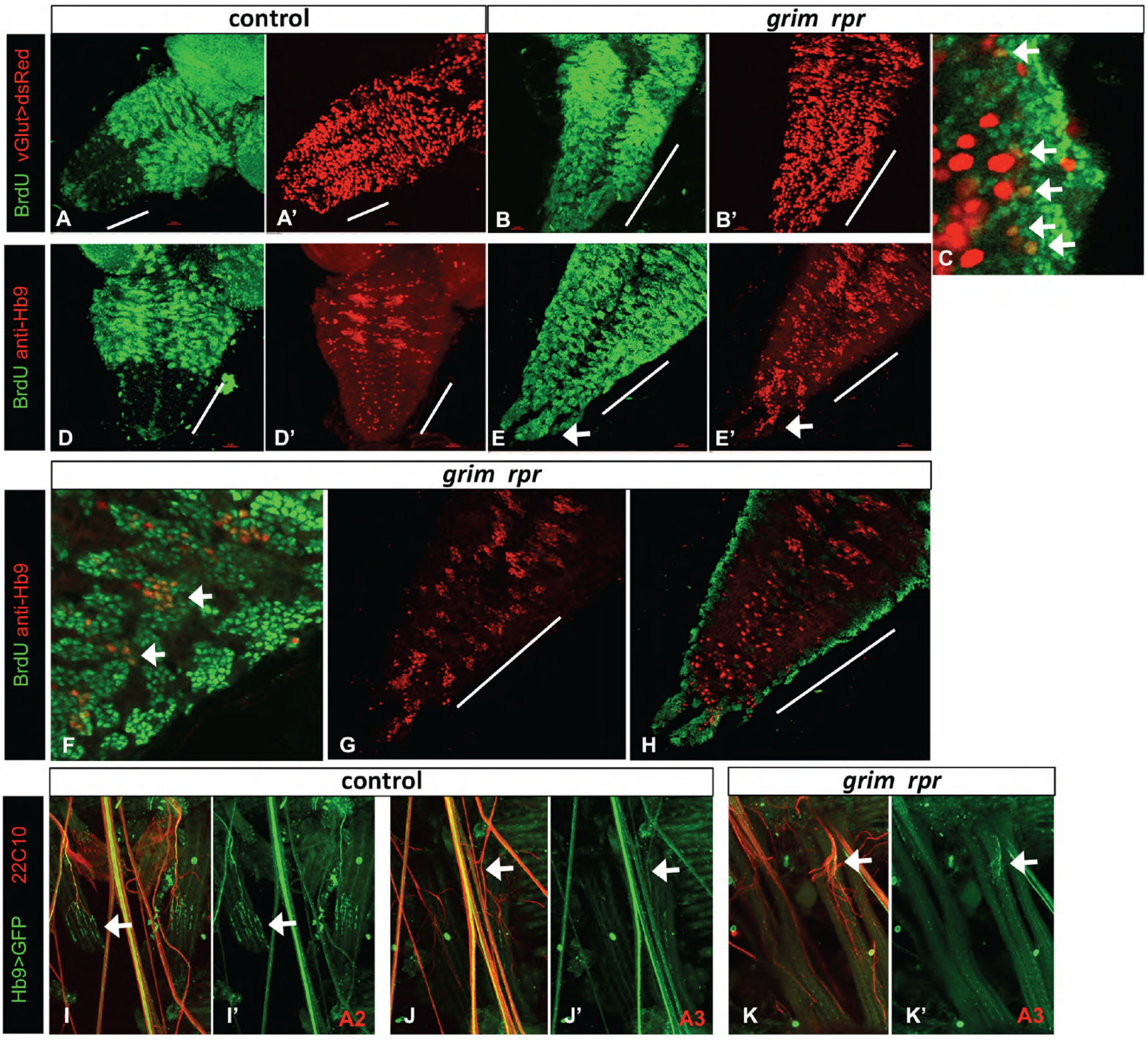

Figure 5. Ectopic vGlut and Hb9 expressing neurons are born post-embryonically in the *grim rpr* mutant

BrdU feeding of larvae was used to label neurons born post-embryonically. The *grim rpr* mutant (3.5A/MM2) (**B, C, E, F–H**) has a dramatic increase in surviving and proliferating NB lineages in the abdominal segments (marked with a white bar). **A–C**) vGlut-Gal4 UAS-dsRed (red) marks glutamatergic motor neurons and some additional neurons. **A–A')** Control larval VNC. **B–C)** There is an increase in BrdU positive (green) dsRed co-labeled cells in the abdominal segments of the *grim rpr* mutant (**arrows in C**) compared to control. **D–H**) Hb9 expressing neurons (red) are born post-embryonically in the thoracic segments of the wild type VNC and appear in three pairs of clusters (**D**), but not in the abdominal segments (abdominal segments marked with a white bar). In the *grim rpr* mutant, medial clusters of post-embryonically born Hb9 expressing cells are present in each abdominal

segment (**E, arrows in F**), including in the terminal extensions seen in these mutants (arrows in **E, E'**). **G** shows Hb9 alone in double labeled ventrally located post-embryonically born clusters, while **H** shows increased embryonically born, more dorsal Hb9 positive cells. Both are increased in the *grim rpr* mutant. I–K') Innervation of specific segments by Hb9 positive motorneurons. Strong ventral muscle innervation by Hb9 expressing motorneurons can be seen in the second abdominal segment (A2) of control animals **(I–I')**. However, this innervation is much reduced in the third segment (A3) of those same individuals **(J–J')**. Innervation by Hb9 expressing motorneurons in the *grim rpr* mutant is unchanged compared to control **(K–K'** and **J–J')**.

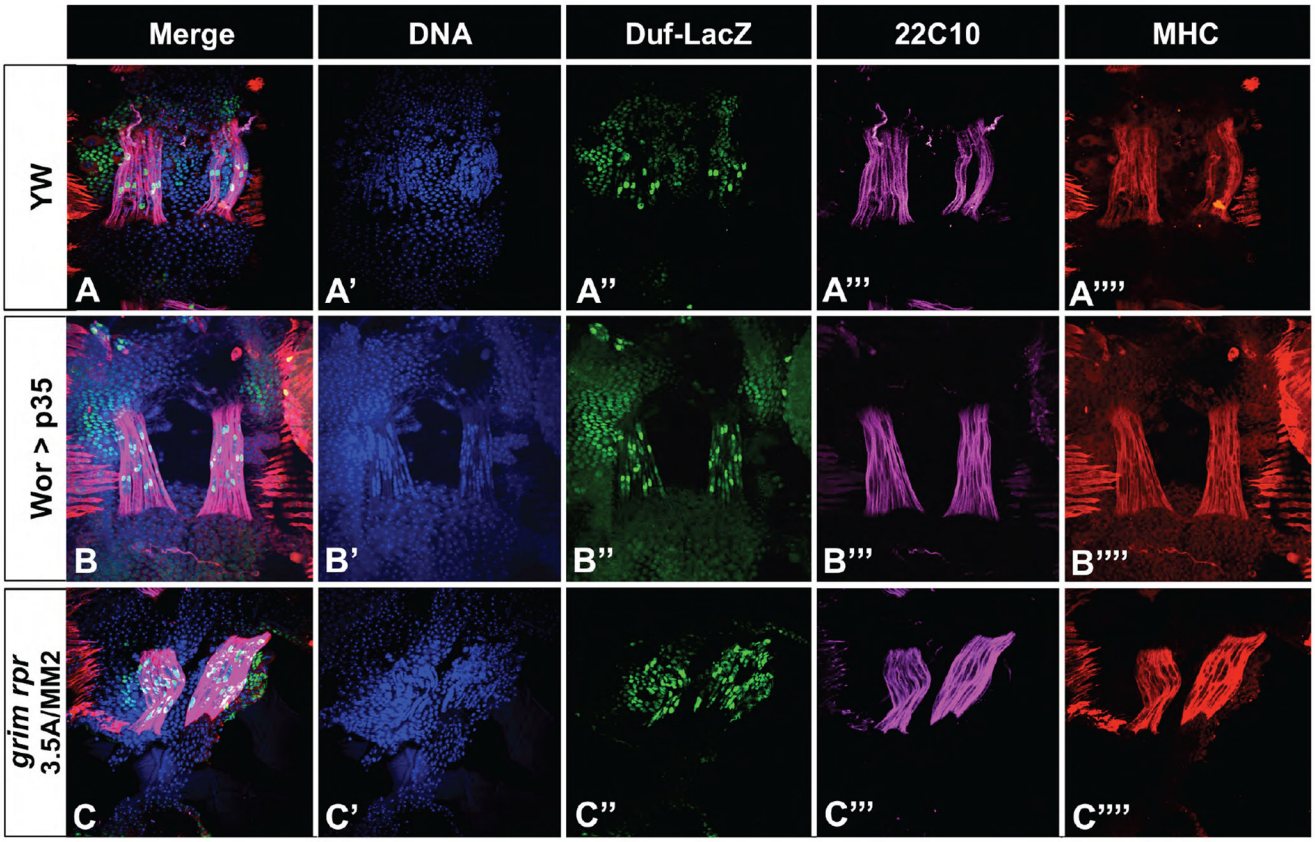

Figure 6. Increased fiber number is due to increased founder cells

Duf-lacZ was used to mark FCs in pupae. At 44 hours APF there is a single duf bright cell in each fiber in all genotypes. Muscle fibers are marked with both anti-22C10 (pink) and anti-MHC (red), DNA is stained with Hoechst 33342 (blue). **A)** Wild type pupal preparation shows a segment that is starting to form fibers. Both wor>p35 (**B**) and the *grim rpr* mutant (**C**) show increased founder cell and fiber number.

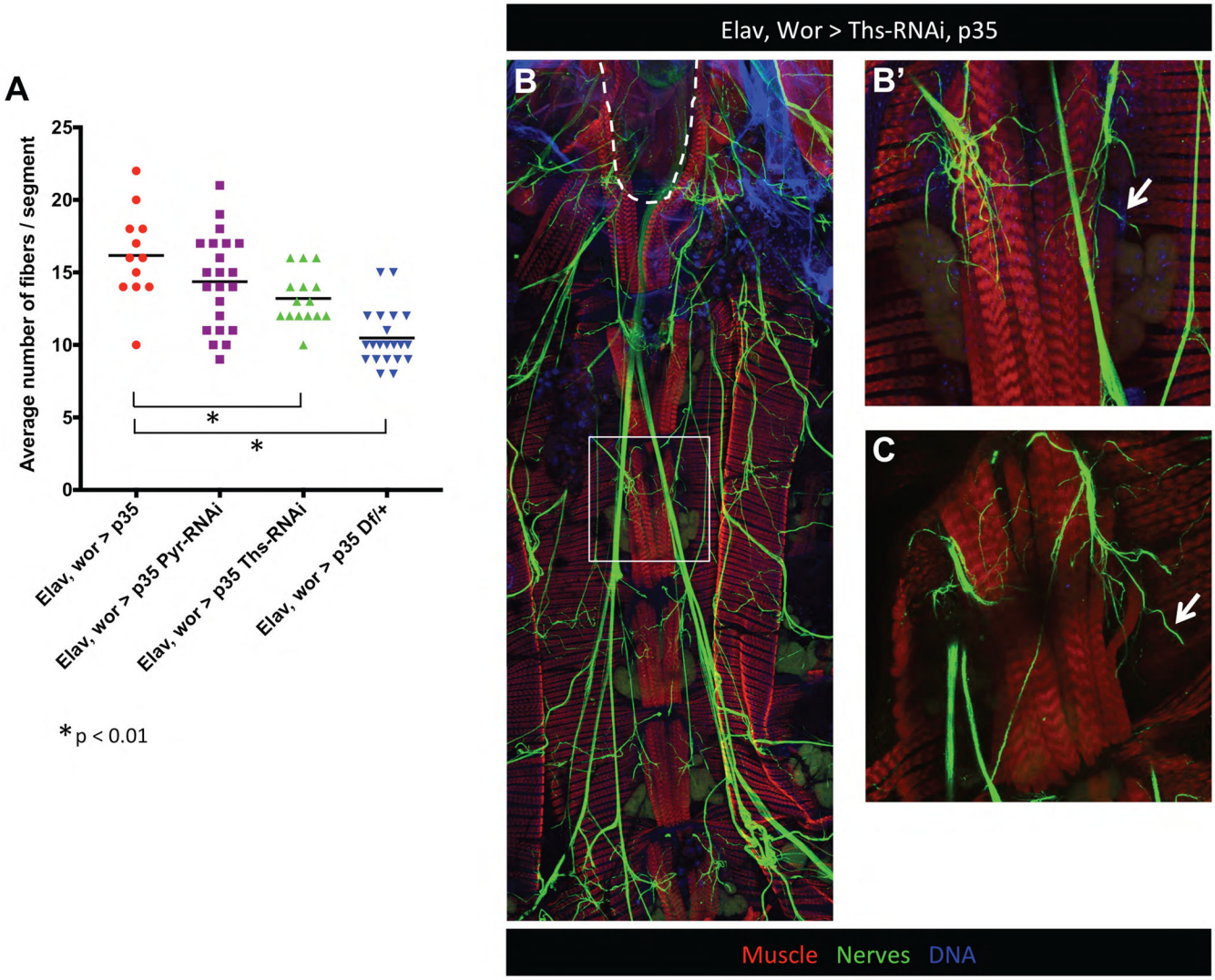

Figure 7. FGFs in the CNS contribute to extra muscle fibers in cell death mutants

A) When cell death is inhibited in in the CNS (elav, wor > p35), on average about 17 fibers are formed per segment. Interfering with the expression of just one FGF ligand in the CNS, significantly reduces the number of fibers to an average of 13 (elav, wor >ths-RNAi, p35, *p<0.01). Heterozygous deletion of both FGF ligands (Df(2R)BSC25/+; wor, elav >p35) reduces the number of fibers per segment to normal levels even when death of neurons and NBs is rescued (* p<0.01). Animals/genotype elav wor>p35 n=4, elav wor>p35 thsRNAi n=4, elav wor>p35 pyrRNAi n=6, elav wor>p35 Df(2R)BSC25/+ n=7. **B)** Although depletion of one FGF ligand in the CNS significantly reduces the number of muscle fibers, the excess innervation seen in elav wor>p35 is still present (Elav, Wor > Ths-RNAi, p35 compared to Elav, wor > p35 in Fig 4C, 4D–D'). However, due to the lack of cell death, neurons that don't innervate muscles in these mutants seem to project aimlessly (arrows in **B'** and **C**).

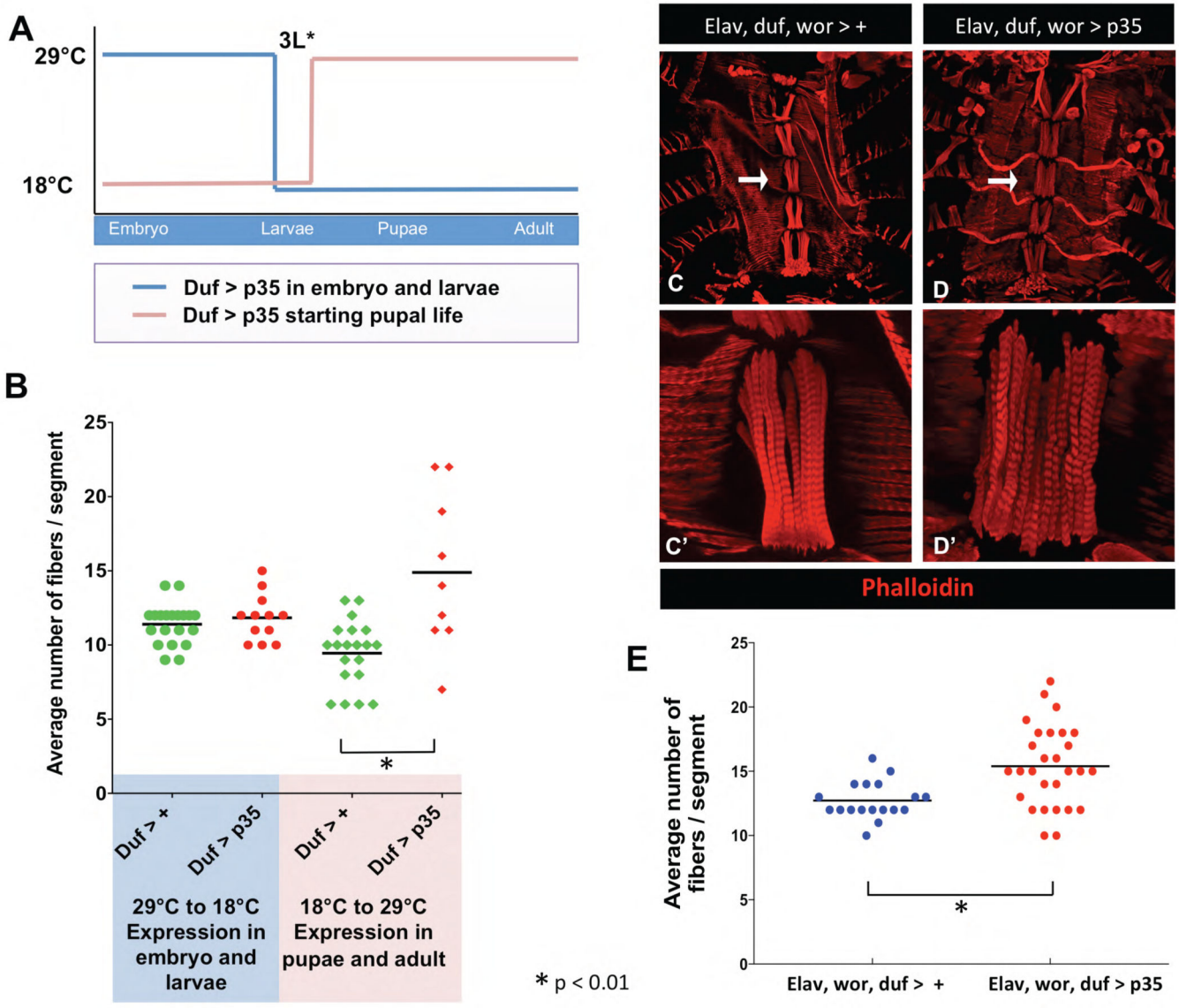

Figure 8. Pupal cell death in founder cells and neurons together limit ventral muscle fiber number

A) A temperature sensitive Gal80 was used to control expression of p35 in Duf-Gal4 expressing cells, allowing expression only in the embryo and larvae, or only in the pupae and adult. Embryos were raised either at 29°C or at 18°C until 3rd instar larvae. Those raised at 29°C were switched to 18°C to stop expression of p35 in pupal and adult life. Alternatively, embryos raised at 18°C were switched to 29°C to activate the expression of p35 in pupal and adult FCs. Adults were dissected to observe effects on muscle fiber number. **B**) There was no alteration in ventral fiber numbers in the adult when p35 was expressed in embryos and larvae, but expression starting in pupae resulted in a significant increase in muscle fiber numbers ($\bar{x}$ shown as bar,*$p \leq 0.001$). **C–E)** Blocking cell death simultaneously in the neurons, NBs and FCs results in a significant increase in fiber number. Control animals containing three drivers: elav-Gal4, duf-Gal4 and wor-Gal4, entire abdomen shown at 10X **(C)** arrow shows the segment imaged in **C'** at 60X. Using all three drivers to

express p35 results in a dramatic increase in number of fibers, with a large animal to animal variation (**D)** quantified in **E** ($\bar{x}$ shown as bar,*$p \leq 0.001$).